N-Phenyl[60]fulleropyrrolidines: PC61BM-Alternative Acceptor Material for High Performance Organic Photovoltaic Cells

Journal:	*Journal of Materials Chemistry A*
Manuscript ID:	TA-ART-09-2014-004857.R1
Article Type:	Paper
Date Submitted by the Author:	23-Oct-2014

Complete List of Authors:	Karakawa, Makoto; Osaka university, The institute of scientific and industrial research Nagai, Takabumi; Daikin Industries LTD, Adachi, Kenji; Daikin Industries LTD, Ie, Yutaka; Osaka University, The Institute of Scientific and Industrial Research Aso, Yoshio; Osaka University, The Institute of Scientific and Industrial Research

Journal Name

RSCPublishing

ARTICLE

N-Phenyl[60]fulleropyrrolidines: $PC_{61}BM$-Alternative Acceptor Material for High Performance Organic Photovoltaic Cells

Cite this: DOI: 10.1039/x0xx00000x

Received 00th January 2012,
Accepted 00th January 2012

DOI: 10.1039/x0xx00000x

www.rsc.org/

Makoto Karakawa,[a] Takabumi Nagai,[b] Kenji Adachi,[b] Yutaka Ie [a] and Yoshio Aso[a,]†,

A series of novel soluble [60]fulleropyrrolidine derivatives bearing relatively simple substituents like [6,6]-phenyl C_{61} butyric acid methyl ester ($PC_{61}BM$) is synthesized by using Prato reaction conditions. The photoabsorption and electrochemical properties of the fulleropyrrolidines are investigated to elucidate their molecular-level electronic properties similar to those of $PC_{61}BM$. The investigations of the fulleropyrrolidines as electron acceptors based on bulk-heterojunction type organic photovoltaic (OPV) devices fabricated with P3HT as a donor show clear differences in performance depending on the substituents, and the devices based on the *N*-phenyl[60]fulleropyrrolidine derivatives exhibit good power conversion efficiencies (PCEs) comparable to, or even higher than, that of the standard $PC_{61}BM$-based device. Finally, the OPV devices based on a low-bandgap donor polymer (PTB7) with the *N*-phenyl[60]fulleropyrrolidines show high PCEs up to 7.3%, which is the highest class of performance among [60]fullerene-based OPV devices, indicating that *N*-phenyl[60]fulleropyrrolidine derivatives are a promising alternative to $PC_{61}BM$ for OPV acceptor materials.

Introduction

Tremendous efforts have been devoted to achieving high efficiencies in organic photovoltaic (OPV) cells consisting of organic electron-donor and electron-acceptor materials.[1] OPV cells have several advantages over silicon solar cells, such as solution processability, mechanical flexibility, and potential low-cost large module fabrication,[1,2] even though OPV cells exhibit still lower power conversion efficiencies (PCEs) than silicon solar cells. A soluble buckminsterfullerene derivative, [6,6]-phenyl C_{61} butyric acid methyl ester ($PC_{61}BM$), has been most widely used as a standard electron-acceptor material for bulk-heterojunction (BHJ) type OPV cells.[1-3] The PCEs of the BHJ solar cells based on a blend of $PC_{61}BM$ with regioregular poly(3-hexylthiophene) (P3HT), a typical donor polymer material, have now reached as high as 6%.[3,4] Furthermore, a rapid increase in the PCEs has been recently caused by the development of a wide variety of new donor polymers having a narrow optical band gap and a low-lying energy level of the highest occupied molecular orbital (HOMO), which contribute to utilizing a broader range of solar light and gaining a higher open-circuit voltage, respectively.[1,5] On the other hand, most of reported high-performance BHJ solar cells have been fabricated using $PC_{61}BM$ or its C_{70} analog, $PC_{71}BM$, as the acceptor material, since they were used in the first reports.[6,7] This narrow structural diversity in the acceptor materials leads to insufficient fundamental understanding of OPV, limiting further performance improvement, and reduction in practical production costs.[8] Thus new alternative electron acceptors suitable to BHJ-type OPVs have been keenly sought in fullerene derivatives as well as non-fullerene materials.

Several $PC_{61}BM$-analogous methano[60]fullerenes with modified solubility in processing solvents, modified affinity with donor polymers, and regulated energy levels of the lowest unoccupied molecular orbital (LUMO) were synthesized via replacement of the phenyl group with other aromatic derivatives, replacement of the methyl ester group with several longer- or branched-alkyl ester groups, replacement of the bridged carbon atom with hetero atoms, or bis- and multi-addition of the methylene bridge, and were tested for applicability to BHJ-type OPVs.[9-15] In contrast, there are a few other fullerene derivatives that have been applied to OPVs. Bis(silylmethyl)[60]fullerenes[16] and indene[17] and dihydromethylene[18] multi-adducts of fullerene achieved successfully high performances on their OPV cells by a combination with tetrabenzoporphyrin and P3HT donors, respectively. Compared with these fullerene derivatives, fulleropyrrolidines have the advantages in a chemical viewpoint, e.g. simple one-step synthetic procedure using Prato reaction conditions from pristine fullerene,[19] easy modification of the substituents linked to the pyrrolidine ring by using commercially available or easily prepared glycine and aldehyde derivatives as reactants, and higher chemical stability of the pyrrolidine structure than that of the tree-membered ring against the corresponding retro-cyclization reactions;[20] nevertheless, fulleropyrrolidine derivatives have not been attracted much attentions because the performances of their based OPV cells remain at an insufficient level.[21] To the best of our knowledge, precedents for the fulleropyrrolidines that showed a performance as good as $PC_{61}BM$ as the OPV acceptor are limited to recently reported *N*-methoxyethoxyethyl-2-aryl[60]fulleropyrrolidines[22a,22b] and indole-containing fulleropyrrolidine derivatives.[22c] Taking this situation into consideration, we have rigorously investigated the OPV performances of [60]fulleropyrrolidine derivatives bearing relatively simple substituents like $PC_{61}BM$. In this paper, we report on the synthesis and electronic properties of novel [60]fulleropyrrolidines and on the characteristics of their based OPV cells in comparison with those of the corresponding $PC_{61}BM$-based cells. Consequently, the performance data of BHJ-type OPV cells fabricated from the synthesized [60]fulleropyrrolidines with P3HT as an electron donor revealed that *N*-phenyl-substituted [60]fulleropyrrolidine derivatives are good OPV acceptors comparable to $PC_{61}BM$. Finally, the high potential of the *N*-phenyl[60]fulleropyrrolidines as n-type OPV materials is demonstrated by improved performances on a combination with a low-band-gap p-type polymer, thieno[3,4-*b*]thiophene/benzodithiophene (PTB7).[5] These OPV performances are the highest class among the cells based on [60]fullerene derivatives. Considering their easy synthesis, *N*-phenyl[60]fulleropyrrolidine derivatives are to be a promising alternative to $PC_{61}BM$.

Results and discussion

Synthesis of fulleropyrrolidine derivatives

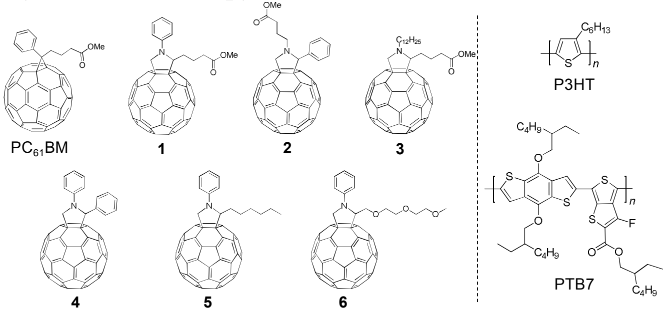

Figure 1. Chemical structures of acceptor materials: $PC_{61}BM$ and [60]fulleropyrrolidine derivatives **1**–**6**, and donor materials: P3HT and PTB7.

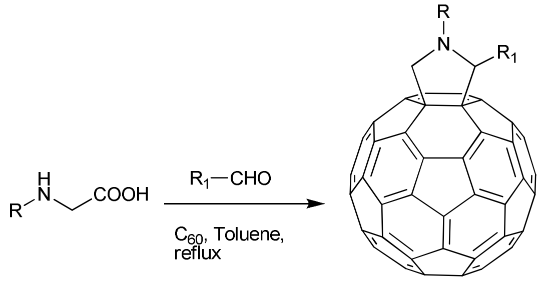

1: R = Ph, $R_1 = (CH_2)_3CO_2CH_3$ (37%)
2: $R = (CH_2)_3CO_2CH_3$, R_1 = Ph (12%)
3: $R = C_{12}H_{25}$, $R_1 = (CH_2)_3CO_2CH_3$ (47%)
4: R = Ph, R_1 = Ph (34%)
5: R = Ph, $R_1 = C_6H_{13}$ (25%)
6: R = Ph, $R_1 = CH_2O(C_2H_4O)_2CH_3$ (40%)

Scheme 1. Synthesis of [60]fulleropyrrolidine derivatives **1**–**6**.

Novel [60]fulleropyrrolidine derivatives **1**–**6** investigated in this work are shown in Figure 1. Their chemical structures were designed to make consecutive variations from a $PC_{61}BM$ analogue. Compounds **1** and **2** are analogous to $PC_{61}BM$ in their substituents with replacing the cyclopropane ring to a pyrrolidine ring. The replacing the *N*-phenyl group in **1** with a dodecyl group leads to the structure of a typical *N*-alkylfulleropyrrolidine derivative **3**. On the other hand, the replacement of the methyl butyrate group at *C*-2 on the pyrrolidine ring of **1** with phenyl, hexyl, and 2,5,8-trioxanonyl substituents leads to a series on *N*-phenyl derivatives **4**, **5**, and **6**, respectively. The synthetic method for these [60]fulleropyrrolidine derivatives is depicted in Scheme 1,[20] in which the essential stating components, glycine and aldehyde derivatives, were purchased or prepared using conventional synthetic procedures.[23-25] The synthesized [60]fulleropyrrolidine derivatives were purified by recycling preparative gel-permeation chromatography (GPC) eluted with chloroform and then by preparative high performance liquid chromatography (HPLC) using COSMOSIL Buckyprep® columns eluted with toluene, and were obtained as black or brown powders. These [60]fulleropyrrolidines **1**–**6** were soluble in common organic solvents, such as chloroform, chlorobenzene, and *o*-dichlorobenzene, affording good processability for OPV-cell fabrication.

UV-vis absorptions

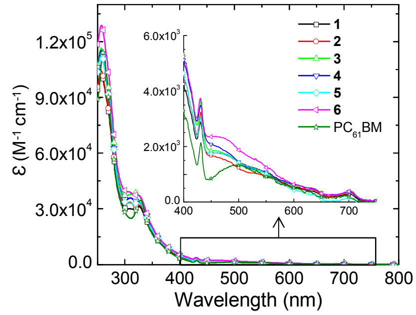

Figure 2. UV−vis absorption spectra of [60]fulleropyrrolidine derivatives **1**–**6** and $PC_{61}BM$ in $CHCl_3$ solutions.

UV−vis absorption spectra of the [60]fulleropyrrolidine derivatives **1**−**6** and $PC_{61}BM$ in chloroform solutions are shown in Figure 2. All the compounds exhibited two characteristic absorption bands between 250 and 350 nm with peak maxima at 257 and 310-320 nm similarly to pristine C_{60}.[26] The [60]fulleropyrrolidines exhibited a weak sharp absorption at 430 nm, which is similarly observed for $PC_{61}BM$ at 431 nm and is distinctive of fulleropyrrolidine and methanofullerene monoadducts.[22,26,27] This absorption is known as a transition originating in partially broken symmetry of the fullerene core[28] and not observed in bisadducts.[29] A weak absorption peak around 700 nm detected in all of the compounds corresponds to the HOMO−LUMO transition of the fullerene core. Overall, it is clear that the different substituent groups on the pyrrolidine ring do not affect the electronic structure of the fullerene π-system because all the spectra were very similar in shape as well as in molar extinction coefficients.

Electrochemical properties

To investigate the electrochemical properties and estimate the LUMO energy levels of the [60]fulleropyrrolidines, cyclic voltammetry (CV) measurements were carried out, together with $PC_{61}BM$ for comparison, using a three-electrode cell in a chlorobenzene/CH_3CN (5/1, v/v) mixed solvent. The LUMO energy levels (E_{LUMO}'s) of the compounds were estimated using the following empirical equation: $E_{\mathrm{LUMO}} = -(E^1_{1/2} + 4.8)$ eV, where $E^1_{1/2}$ is the first half-wave reduction potential relative to the Fe/Fe$^+$.[30] The cyclic voltammograms are shown in Figure S1, and the obtained half-wave potential ($E_{1/2}$) and E_{LUMO} values are summarized in Table

1. The [60]fulleropyrrolidine derivatives underwent two reversible redox processes similarly to $PC_{61}BM$ within a potential window of the measurement, and their first reduction potentials showed a little deviation within ±0.03 V from that of $PC_{61}BM$. Therefore, the LUMO energy levels of the [60]fulleropyrrolidine compounds were little affected by the substituents, though the *C*-2 alkyl and alkyl ether substituted compounds (**5** and **6**) showed slightly higher LUMO energy levels compared with the methyl butyrate or phenyl substituted compounds (**1** or **4**). These photophysical and electrochemical measurements clearly indicate that the molecular-level electronic properties of the [60]fulleropyrrolidine derivatives are quite similar to those of $PC_{61}BM$.

Table 1. Reduction potentials and estimated LUMO energy levels of [60]fullerene derivatives.

Compound	$E^{1}_{1/2}$ (V vs Fe/Fe^{+})	$E^{2}_{1/2}$ (V vs Fe/Fe^{+})	E_{LUMO} (eV)[a)]
1	–1.12	–1.50	–3.68
2	–1.11	–1.51	–3.69
3	–1.12	–1.54	–3.68
4	–1.13	–1.53	–3.67
5	–1.14	–1.57	–3.66
6	–1.16	–1.57	–3.64
$PC_{61}BM$	–1.13	–1.51	–3.67

[a)] Values estimated from first reduction potentials.

OPV performances

The properties of BHJ-type OPV cells fabricated from the present [60]fulleropyrrolidine derivatives as acceptor materials and P3HT as a donor material were investigated with a standard device structure of ITO/PEDOT-PSS/active layer/Al, in which PEDOT-PSS is poly(3,4-ethylenedioxythiophene)-poly(styrenesulfonate) as a buffer layer. Conditions for the fabrication of BHJ active layers were optimized on solvent and concentration for spin-coating, donor–acceptor (D/A) ratio, and annealing temperature (see Experimental). The current–voltage (*J*–*V*) characteristics of the optimized OPV cells measured under simulated AM 1.5 G solar irradiation at 100 mW/cm^2 are shown in Figure 3, and their photovoltaic performance data including a short-circuit current (J_{sc}), open-circuit voltage (V_{oc}), fill factor (FF), and the PCE are summarized in Table 2. Interestingly, the PCEs ranged largely from 0.02% to 2.41% depending on the substituents of the [60]fulleropyrrolidine derivatives. Under the same device structure and measurement conditions, the $PC_{61}BM$-based reference cell exhibited a PCE of 2.30% (Table 2). The OPV device using compound **1** exhibited a moderate PCE of 1.83%. In contrast, the device based on compounds **2** showed low J_{sc}, low V_{oc}, and low FF values, resulting in a poor PCE of 0.21%, despite its similar chemical structure to compound **1** with only the difference of substituent positions on the pyrrolidine ring. Moreover, when the phenyl substituent at *N*-1 position in compound **1** was replaced with a dodecyl group in compound **3** to enhance the solubility, the device based on **3** exhibited substantially low OPV performance with a PCE of 0.02%. The *J*–*V* characteristics of these low-PCE devices based on **2** and **3** showed S-shaped features (Figure 3) that lead to their low FF and J_{sc} values. These findings confirm a critical dependence of the device performance on the chemical structures of the [60]fulleropyrrolidine derivatives, and it appears that the *N*-phenyl group has a positive effect. Indeed, OPV cells fabricated using the *N*-phenyl derivatives **4**, **5**, and **6** exhibited relatively good performances as shown in Table 1. The highest performance was marked by the OPV cell based on compound **4**, which has phenyl groups at both the *N*-1 and *C*-2 positions of the pyrrolidine ring, exhibiting J_{sc} of 8.309 mA/cm^2, V_{oc} of 0.594 V, FF of 0.488, and the resulting PCE of 2.41%. It is noteworthy that the OPV performances of the cells based on these *N*-phenyl[60]fulleropyrrolidines **4**–**6** are comparable to, or even higher than, that of the standard $PC_{61}BM$-based cell.

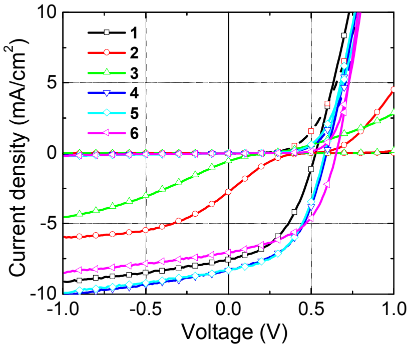

Figure 3. *J*–*V* characteristics of OPV cells based on blends of P3HT and [60]fulleropyrrolidine derivatives **1**–**6**.

Table 2. Performance parameters of organic photovoltaic cells based on P3HT and [60]fullerene derivatives.

Acceptor	D/A	J_{sc} (mA/cm^2)	V_{oc} (V)	FF	PCE (%)[a]
1	1:1	7.560	0.528	0.458	1.83 (1.65)
2	1:1	2.751	0.478	0.156	0.21 (0.15)
3	1:1	0.535	0.226	0.180	0.02 (0.01)
4	1.5:1	8.309	0.594	0.488	2.41 (2.07)
5	1:1	8.308	0.583	0.493	2.39 (2.05)
6	1:1	7.061	0.652	0.509	2.34 (1.86)
$PC_{61}BM$	1.5:1	7.307	0.603	0.521	2.30 (2.06)

[a)] Averaged values in parentheses.

Atomic force microscopy (AFM) measurements were carried out to investigate the surface morphologies of the blend films consist of the fullerene derivatives and P3HT. As shown in Figure S2, all films appeared to have substantially well-blended structures and displayed a root-mean-square roughness of less than 5 nm. In detailed comparison of the AFM images, all the fulleropyrrolidine-based blend films exhibited similar-sized or slightly large-sized (P3HT/**1**: Figure S2a) grain morphologies compared with the P3HT/$PC_{61}BM$ blend film (Figure S2h). Thus, no clear correlation between the film morphologies and the OPV performances is observed. These well-blended film morphologies indicate that the synthesized [60]fulleropyrrolidine derivatives have achieved miscibility with P3HT, which is one of the important requirements for OPV applications of acceptor materials. Although several causes are supposed,[31] the S-shaped *J*–*V* curves observed in the low-PCE OPV cells based on *N*-alkyl[60]fulleropyrrolidines **2** and **3** might be partially caused by high series resistances resulting from undesirable interactions between the highly basic *N*-alkylpyrrolidine and strongly acidic PSS comprised in the buffer layer.[22b] This was supported by the fact that the performances of compound **2** and **3** based devices were improved by using a MoOx buffer layer instead of PEDOT:PSS to PCEs of 1.44% and 0.54%, respectively, whereas, on the same device structure, no improvement of the PCE for **1** based device was observed (Figure S3 and Table S1 in ESI).

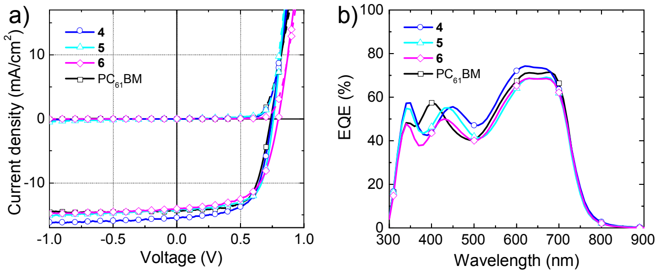

Figure 4. OPV cell performance using PTB7 as a donor and compounds **4**–**6** as an acceptor; a) *J*-*V* curves and b) EQE spectra together with those of PC$_{61}$BM-based device [**4**: open circle, **5**: open triangle, **6**: empty diamond, and PC$_{61}$BM: open square].

Table 3. Performances of OPVs using PTB7 as a donor material

Acceptor	J_{sc} (mA/cm^2)	V_{oc} (V)	FF	PCE (%)[a]
4	15.483	0.749	0.633	7.34 (6.93)
5	14.208	0.760	0.673	7.27 (7.06)
6	14.033	0.797	0.610	6.83 (6.51)
PC$_{61}$BM	14.292	0.740	0.665	7.03 (6.80)

[a] Averaged values (**4**, **5**, and **6**: 8 devices; PC$_{61}$BM: 7 devices) in parentheses.

For further improvements of OPV performance and demonstrating the potential of the *N*-phenyl[60]fulleropyrrolidine derivatives **4**–**6** as the accepter materials, we fabricated the OPV cells using a combination with PTB7 (the chemical structure is shown in Figure 1),[5] which is a commercially available low-band-gap p-type polymer. In addition, a following inverted device structure,[32] which is advantageous to device durability,[33] was applied: ITO/PFN/active layer/MoO$_x$/Al, in which PFN is poly [(9,9-bis(3'-(*N*,*N*-dimethylamino)propyl)-2,7-fluorene)-alt-2,7-(9,9–dioctylfluorene)] used as a cathode interlayer.[32,34] A PC$_{61}$BM-based cell with the same device structure was also fabricated for comparing the performances. The active layer was spin-coated on the PFN layer from a chlorobenzene solution of the PTB7/acceptor (1/1.5 weight ratio) blend including 3% 1,8-diiodooctane (DIO) in a nitrogen atmosphere. As shown in Figure 4, the *J*–*V* curves and external quantum efficiency (EQE) spectra of the devices based on *N*-phenyl[60]fulleropyrrolidines **4**–**6** were almost identical to those of the PC$_{61}$BM-based device. Their performance data are summarized in Table 3. The **4**-based device exhibited a higher J_{sc} compared with other devices, whereas the devices using *C*-2-alkylated **5** and **6** showed apparently higher V_{oc} values than the **4**-based and PC$_{61}$BM-based devices, probably reflecting their slightly higher LUMO energy levels (Table 1).[35] Overall, the device using the PTB7/**4** blend film exhibited the highest PCE of 7.34% among these devices. It is well worth noting that the PCE values for PTB7/**4** and PTB7/**5** blends are higher than that for the PTB7/PC$_{61}$BM blend. The AFM images of these blend films shown in Figure S3 revealed similar roughness and grain sizes to the PTB7/PC$_{61}$BM blend film, suggesting the formation of a nano-size phase-separated structure proper for obtaining high BHJ OPV performances. From careful observation, the PTB7/**6** blend film was found having a slightly smaller grain structure, which might affect its slightly low J_{sc} and FF values.

Conclusions

In conclusion, we have synthesized novel [60]fulleropyrrolidine derivatives and investigated their detailed electronic absorption, electrochemical, and photovoltaic properties. Though the absorption and electrochemical properties of all these compounds closely resemble each other and those of PC$_{61}$BM, BHJ OPV cells fabricated using the [60]fulleropyrrolidines as acceptor materials and P3HT as a donor material demonstrated clearly varied performances according to the substituents on the pyrrolidine ring. The OPV cells based on the *N*-alkyl-substituted fulleropyrrolidines **2** and **3** exhibited low performances, while the performances obtained from the cells using the *N*-phenyl fulleropyrrolidine derivatives **4**, **5**, and **6** were comparable or even higher compared with that of the corresponding PC$_{61}$BM-based cell. This result indicates that the presence of the *N*-phenyl group has a positive effect to OPV performances. Furthermore, we fabricated the OPV devices using these *N*-phenyl [60]fulleropyrrolidines with a typical low-band gap polymer (PTB7) as a donor material, and found that these devices exhibited excellent performances. Note that both the performances of the **4**- and **5**-based cells exceed that of the corresponding PC$_{61}$BM-based cell, suggesting the high potential of the *N*-phenyl[60]fulleropyrrolidine derivatives. Although, Tan et al. recently reported 8.75% efficiency using a low-band-gap p-type polymer (PBDTBDD) and PC$_{61}$BM,[36] the PCE of 7.34% obtained from the PTB7/**4** blend is still the world highest class performance among [60]fullerene-based OPV cells.[37] Considering their easy synthesis, *N*-phenyl[60]fulleropyrrolidine derivatives are a promising alternative to PC$_{61}$BM for OPV acceptor materials.

Experimental

Materials

Reagents were purchased from Wako Pure Chemical Industries, Tokyo Kasei Chemical Industries, Merck Ltd., and Aldrich, and used without further purification. [60]Fullerene was purchased from Honjo Chemical Corporation. P3HT was purchased from Merck Ltd. PTB7 as a donor material for OPV cells was purchased from 1-material Chemscitech and used as received. PFN was synthesized in accordance with literature procedures.[34]

General Measurement and Characterization

UV–vis absorption spectra were recorded on Shimadzu UV-3100PC. All spectra were obtained in spectrograde solvents using quartz cells with a 1 cm path length. ^{1}H and ^{13}C NMR spectra were recorded with a JEOL JNM-ECS400 (400 MHz for ^{1}H and 100 MHz for ^{13}C) spectrometer in chloroform-*d* [chemical shifts were reported in parts per million (ppm) downfield from tetramethylsilane as an internal standard]. Cyclic voltammetry was carried out on a BAS CV-50W voltammetric analyzer using Pt working and counter electrodes in a chlorobenzene/CH_3CN (5/1, v/v) solution containing 0.1 mol/L Bu_4NPF_6. Column chromatography was performed on silica gel, KANTO Chemical silica-gel 60N (40–50 μm). Synthesized [60]fulleropyrrolidine compounds were purified with recycling GPC with the use of Japan Analytical Industry LC-908 equipped with JAI-GEL 1H/2H columns (eluent: $CHCl_3$) and then with recycling HPLC using COSMOSIL Buckyprep® columns (eluent: toluene). Elemental analyses were performed on Perkin Elmer LS-50B by the Elemental Analysis Section of Comprehensive Analysis Center (CAC), ISIR, Osaka University. Surface morphologies of deposited organic films were observed using an atomic force microscope (Shimadzu, SPM9600). The thicknesses of deposited organic films were measured using KLA-Tencor alpha-step IQ surface measurement profiler.

Typical synthetic procedure

C_{60}-fused *N*-phenyl-2-phenylpyrrolidine (**4**)

A toluene solution (100 mL) of benzaldehyde (28.5 mg, 0.25 mmol), *N*-phenylglycine (76 mg, 0.5 mmol), and [60]fullerene (175 mg, 0.25 mmol) was stirred at 110 °C for 24 h under a nitrogen atmosphere and concentrated under reduced pressure. The product was separated by column chromatography (SiO_2, *n*-hexane:toluene, 10:1) to give the compound **4** (78 mg, 34%), which was further purified with preparative recycling GPC and then HPLC; ^{1}H NMR (400 MHz, $CDCl_3$, δ): 5.00 (1H, d, J = 10.5 Hz), 5.68 (1H, d, J = 10.5 Hz), 6.08 (1H, s), 7.02-7.10 (1H, m), 7.22-7.40 (7H, m), 7.70-7.81 (2H, m). ^{13}C NMR (100 MHz, $CDCl_3$, δ): 68.21, 68.61, 121.50, 122.37, 128.26, 128.65, 128.84, 129.19, 135.72, 135.80, 136.54, 137.79, 139.35, 139.89, 140.21, 140.30, 141.58, 141.75, 141.86, 141.91, 142.06, 142.07, 142.12, 142.15, 142.18, 142.27, 142.28, 142.63, 142.74, 143.06, 143.19, 144.45, 144.62, 144.73, 145.18, 145.29, 145.32, 145.36, 145.48, 145.49, 145.61, 145.75, 146.00, 146.09, 146.14, 146.19, 146.28, 146.29, 146.30, 146.40, 146.68, 153.27, 153.46, 153.80, 155.82; UV–vis ($CHCl_3$): λ_{max} (ε) = 257 nm (115000); MS (FAB) m/z 916 (M+1): HRMS calcd for $C_{74}H_{13}N$: 915.10480; found: 915.1039; the sample for elemental analysis was obtaind as **4**:toluene = 1:1, which was confirmed by its ^{1}H NMR spectrum, Anal. Calcd. for $C_{81}H_{21}N$: C 96.51, H 2.10, N 1.39; Found: C 96.46, H 2.01, N 1.53.

OPV device fabrication and measurements

Patterned ITO on a glass slide (Sanyo Vacuum Industries Co., Ltd.) was treated in an O_2-plasma oven for 5 min. Thereafter, a PEDOT-PSS layer is prepared on the ITO-coated grass slide by spin-coating (500 rpm for 5 s and then 3000 rpm for 60 s) of a filtered (0.45 μm pore size PTFE membrane filter) aqueous suspension of PEDOT-PSS (Clevios P VP Al 4083), and then baked at 135 °C for 10 min in the air. Poly(3-hexylthiophene) (P3HT) (Merck Ltd.) and the fullerene derivative was dissolved in chlorobenzene at room temperature and then spin coated on the top of the PEDOT-PSS layer at 1500 rpm for 60 s. The thicknesses of the resulting P3HT/acceptor films were found to be ca. 130 nm. The device fabrication was completed by the vacuum deposition of Al cathode (ca. 80 nm) through a shadow mask, which defined the active area of each OPV device to be 3×3 mm^2. The device was thermally annealed for 10 min prior to performance measurement; optimized annealing temperature is 80 °C for **1**, 80 °C for **2**, no-annealed for **3**, 130 °C for **4**, 130 °C for **5**, no-annealed for **6**, and 130 °C for $PC_{61}BM$.

For the inverted device structure of ITO/PFN/PTB7:acceptor/MoO_x/Al, the PFN interlayer material was dissolved in methanol (concentration, 2 mg/mL) in the presence of a small amount of acetic acid was spin-coated on top of the precleaned ITO substrate in accordance with literature conditions.[32,34] The organic active layer, with a thickness of 90–100 nm, was prepared by spin coating from a blend solution (concentration, 25 mg/mL) in chlorobenzene including 1,8-diiodoctane (3%) at 1,000 rpm for 2 min in a nitrogen atmosphere. A 10-nm MoO_x layer and a 80-nm Al layer were successively evaporated in a vacuum chamber through a shadow mask to form a top anode with defining the active area of the devices (3 × 3 mm^2).

The solar cells were subsequently tested under simulated air mass (AM) 1.5 G solar irradiation (100 mW/cm^2, SAN-EI ELECTRIC CO., LTD. XES-301S). Current density–voltage (*J–V*) characteristics were recorded using a PC-controlled Keithley 2400 source meter.

Acknowledgements

This work was supported by the Adaptable and Seamless Technology Transfer Program through Target-driven R&D (A-step) from the Japan Science and Technology Agency (JST) and by a cooperative research with Daikin Co., Ltd. Thanks are extended to the Comprehensive Analysis Center (CAC), The Institute of Scientific and Industrial Research (ISIR), Osaka University for their assistance in elemental analyses and NMR measurements.

Notes and references

[a] Department of Soft Nanomaterials, Nanoscience and Nanotechnology Center, The Institute of Scientific and Industrial Research (ISIR), Osaka University, 8-1 Mihogaoka, Ibaraki, Osaka 567-0047, Japan, Fax: (+) 81-6-6879-8479

[b] Fundamental Technology Group, Chemical R&D Center, Daikin Industries, LTD, 1-1 Nishi Hitotsuya, Settsu-shi, Osaka, 566-8585, Japan, Fax: (+) 81-6-6349-4751

† Corresponding to Y. Aso; aso@sanken.osaka-u.ac.jp.

Electronic Supplementary Information (ESI) available: experimental information for synthesis of compounds, CV curves, atomic force microscopy images and additional OPV performance data with *J–V* curves. See DOI: 10.1039/b000000x/

1 a) Y. Li, *Acc. Chem. Res.* 2012, **45**, 723; b) P. Kumar, S. Chand, *Prog. Photovolt: Res. Appl.* 2012, **20**, 377; c) L. Bian, E. Zhu, J. Tang, W. Tang, F. Zhang, *Prog. Polym. Sci.* 2012, **37**,1292; d) M. Jørgensen, K. Norrman, S. A. Gevorgyan, T. Tromholt, B. Andreasen, F. C. Krebs, *Adv. Mater.* 2012, **24**, 580; e) H. Zhou, L. Yang, W. You, *Macromolecules* 2012, **45**, 607; f) M. Mayukh, I. H. Jung, F. He, L. Yu, *J. Poly. Sci. B: Poly. Phys.* 2012, **50**, 1057; g) P.-L. T. Boudreault, A. Najari, M. Leclerc, *Chem. Mater.* 2011, **23**, 456; h) H. J. Son, F. He, B. Carsten, L. Yu, *J. Mater. Chem.* 2011, **21**, 18934.

2 a) R. Søndergaard, M. Hösel, D. Angmo, T. T. Larsen-Olsen, F. C. Krebs, *Materials today* 2012, **15**, 36; b) R. R. Søndergaard, M. Hösel, F. C. Krebs, *J. Polym. Sci. B Polym. Phys*. 2013, **51**, 16; c) J. W. Jung, W. H. Jo, *Adv. Funct. Mater*. 2010, **20**, 2355.

3 a) A. Marrocchi, D. Lanari, A. Facchetti, L. Vaccaro, *Ener. Environ. Sci*. 2012, **5**, 8457; b) M. T. Dang, L. Hirsch, G. Wantz, *Adv. Mater.* 2011, **23**, 3597.

4 K. Kim, J. Liu, M. A. G. Namboothiry, D. L. Carroll, *Appl. Phys. Lett.* 2007, **90**, 163511.

5 a) Y. Liang, Z. Xu, J. Xia, S.-T. Tsai, Y. Wu, G. Li, C. Ray, L. Yu, *Adv. Mater*. 2010, **22**, E135; b) H.-Y. Chen, J. Hou, S. Zhang, Y. Liang, G. Yang, Y. Yang, L. Yu, Y. Wu, G. Li, *Nat. Photo*. 2009, **3**, 649; c) Y. Liang, D. Feng, Y. Wu, S.-T. Tsai, G. Li, C. Ray, L. Yu, *J. Am. Chem. Soc.* 2009, **131**, 7792; d) H. J. Son, W. Wang, T. Xu, Y. Liang, Y. Wu, G. Li, L. Yu, *J. Am. Chem. Soc*. 2011, **133**, 1885.

6 G. Yu, J. Gao, J. C. Hummelen, F. Wudl, A. J. Heeger, *Science* 1995, **270**, 1789.

7 M. M. Wienk, J, M. Kroon, W. J. H. Verhees, J. Knol, J. C. Hummelen, P. A. van Hal, R. A. J. Janssen, *Angew. Chem. Int. Ed.* 2003, **42**, 3371.

8 T .Liu, A. Troisi, *Adv. Mater*. 2013, **25**, 1038.

9 L. Zheng, Q. Zhou, X. Deng, M. Yuan, G. Yu, Y. Cao, *J. Phys. Chem. B* 2004, **108**, 11921.

10 M. Lenes, G-J. A. H. Wetzelaer, F. B. Kooistra, S. C. Veenstra, J. C. Hummelen, P. W. M. Blom, *Adv. Mater.* 2008, **20**, 2116.

11 S. H. Park, C. Yang, S. Cowan, J. K. Lee, F. Wudl, K. Lee, A. J. Heeger, *J. Mater. Chem*. 2009, **19**, 5624.

12 C. Yang, J. Y. Kim, S. Cho, J. K. Lee, A. J. Heeger, F. Wudl, *J. Am. Chem. Soc*. 2008, **130**, 6444.

13 a) P. A. Troshin, H. Hoppe, J. Renz, M. Egginger, J. Y. Mayorova, A. E. Goryachev, A. S. Peregudov, R. N. Lyubovskaya, G. Gobsch, N. S. Sariciftci, V. F. Razumov, *Adv. Funct. Mater.* 2009, **19**, 779; b) P. A. Troshin, E. A. Khakina, M. Egginger, A. E. Goryachev, S. I. Troyanov, A. Fuchsbauer, A. S. Peregudov, R. N. Lyubovskaya, V. F. Razumov, N. S. Sariciftci, *ChemSusChem* 2010, **3**, 356.

14 G. Zhao, Y. He, Z. Xu, J. Hou, M. Zhang, J. Min, H.-Y. Chen, M. Ye, Z. Hong, Y. Yang, Y. Li, *Adv. Funct. Mater*. 2010, **20**, 1480.

15 Y. Morinaka, M. Nobori, M. Murata, A. Wakamiya, T. Sagawa, S. Yoshikawa, Y. Murata, *Chem. Commun.* 2013, **49**, 3670.

16 a) Y. Matsuo, A. Iwashita, Y. Abe, C.-Z. Li, K. Matsuo, M. Hashiguchi, E. Nakamura, *J. Am. Chem. Soc*. 2008, **130**, 15429; b) Y. Matsuo, Y. Sato, T. Niinomi, I. Soga, H. Tanaka, E. Nakamura, *J. Am. Chem. Soc*. 2009, **131**, 16048.

17 a) Y. He, H.-Y Chen, J. Hou, Y. Li, *J. Am. Chem. Soc*. 2010, **132**, 1377; b) G. Zhao, Y. He, Y. Li, *Adv. Mater*. 2010, **22** 4355; c) Y. He, G. Zhao, B. Peng, Y. Li, *Adv. Funct. Mater*. 2010, **20**, 3383.

18 Y. Matsuo, J. Kawai, H. Inada, T. Nakagawa, H. Ota, S. Otsubo, E. Nakamura, *Adv. Mater.* 2013, **25**, 6266.

19 a) M. Maggini, G. Scorrano, M. Prato, *J. Am. Chem. Soc*. 1993, **115**, 9798; b) P. Wang, B. Chen, R. M. Metzger, T. Da Ros, M. Prato, *J. Mater. Chem*. 1997, **7**, 2397.

20 a) N. N. P. Moonen, C. Thilgen, L. Echegoyen, F. Diederich, *Chem. Commun*. 2000, 335; b) N. Martín, M. Altable, S. Filippone, A. Martín-Domenech, *Synlett* 2007, **20**, 3077.

21 a) J.-K. Lee, K. Fujida, T. Tsutsui, M.-R. Kim, *Sol. Energy Mater. Sol. Cells* 2007, **91**, 892; b) P. Wang, K. Yao, L. Chen, Y. Chen, F. Li, H. Wang, S. Yu, *Sol. Energy Mater. Sol. Cells* 2012, **97**, 34; c) B.-Y. Ren, C.-J. Ou, C. Zhang, Y.-Z. Chang, M.-D. Yi, J.-Q. Liu, L.-H. Xie, G.-W. Zhang, X.-Y. Deng, S.-B. Li, W. Wei, W. Hang, *J. Phys. Chem. C* 2012, **116**, 8881; d) D. Mi, H.-U. Kim, J.-H. Kim, F. Xu, S.-H. Jin, D.-H. Hwang, *Synth. Metals* 2012, **162**, 483.

22 a) K. Matsumoto, K. Hashimoto, M. Kamo, Y. Uetani, S. Hayase, M. Kawatsura, T. Itoh, *J. Mater. Chem.* 2010, **20**, 9226; b) K. Yoshimura, K. Matsumoto, Y. Uetani, S. Sakumichi, S. Hayase, M. Kawatsura, T. Itoh, *Tetrahedron* 2012, **68**, 3605; c) X. Zhang, L. Sun, W. Zheng, X. Bao, N. Wang, T. Wang, R. Yang, *Tetrahedron* 2013, **69**, 9544.

23 M. S. Bjelaković, D. M. Godjevac, D. R. Milić, *Carbon*, 2007, **45**, 2260.

24 B. A. Marples, C. G. Saint, J. R. Traynor, *J. Chem. Soc. Perkin Trans 1,* 1986, 567.

25 T. Da Ros, M. Prato, F. Novello, M. Maggini, E. Banfi, *J. Org. Chem*. 1996, **61**, 9070.

26 C. Liu, Y. Li, C. Li, W. Li, C. Zhou, H. Liu, Z. Bo, Y. Li, *J. Phys. Chem. C* 2009, **113**, 21970.

27 a) R. V. Bensasson, E. Bienvenüe, C. Fabre, J.-M. Janot, E. J. Land, S. Leach, V. Leboulaire, A. Rassat, S. Roux, P. Seta, *Chem. Eur. J.* 1998, **4**, 270; b) K. Moriwaki, F. Matsumoto, Y. Takao, D. Shimizu, T. Ohno, *Tetrahedron* 2010, **66**, 7316; c) M. Prato, M. Maggini, *Acc. Chem. Res*. 1998, **31**, 519.

28 a) C. Yang, S. Cho, A. J. Heeger, F. Wudl, *Angew. Chem. Int. Ed*. 2009, **48**, 1592; b) M. Eo, H.J. Bae, M. Hong, Y. Do, S. Cho, M. H. Lee, *Dalton Trans*. 2013, **42**, 8104; c) G. Ye, S. Chen, Z. Xiao, Q. Zuo, Q. Wei, L. Ding, *J. Mater. Chem*. 2012, **22**, 22374.

29 a) G, D, Han, W, R. Collins, T, L. Andrew, V. Bulović, T. M. Swager, *Adv. Funct. Mater*. 2013, **23**, 3061; b) X. Meng, W. Zhang, Z. Tan, C. Du, C. Li, Z. Bo, Y. Li, X. Yang, M. Zhen, F. Jiang, J. Zheng, T. Wang, L. Jiang, C. Shu, C. Wang, *Chem. Commun*. 2012, **48**, 425; c) Y. He, H. Y. Chen. J. Hou, Y. Li, *J. Am. Chem. Soc*. 2010, **132**, 1377.

30 J. Pommerehne, H. Vestweber, W. Guss, R. F. Mahrt, H. Bässler, M. Porsch, J. Daub, *Adv. Mater.* 1995, **7**. 551.

31 O. J. Sandberg, M. Nyman, R. Österbacka, *Phys. Rev. Appl.* 2014, **1**, 024003.

32 Z. He, C. Zhong, S. Su, M. Xu, H. Wu, Y. Cao, *Nat. Photo*. 2012, **6**, 591.

33 T. Kuwabara, T. Nakayama, K. Uozumi, T. Yamaguchi, K. Takahashi, *Sol. Energy Mater. Sol. Cells* 2008, **92**, 1476.

34 F. Huang, H. Wu, D. Wang, W. Yang, Y. Cao, *Chem. Mater*. 2004, **16**, 708.

35 a) C. J. Brabec, A. Cravino, D. Meissner, N. S. Sariciftci, T. Fromherz, M. T. Rispens, L. Sanchez, J. C. Hummelen, *Adv. Funct. Mater*. 2001, **11**, 374; b) M. C. Scharber, D. Mühlbacher, M. Koppe, P. Denk, C. Waldauf, A. J. Heeger, C. J. Brabec, *Adv. Mater*. 2006, **18**, 789.

36 Z.-a. Tan, S. Li, F. Wang, D. Qian, J. Lin, J. Hou Y. Li, *Sci. Rep*. 2014, **4**, 4691.

37 a) H. Zhou, L. Yang, A. C. Stuart, S. C. Price, S. Liu, W. You, *Angew. Chem. Int. Ed.* 2011, **50**, 2995; b) S. C. Price, A. C. Stuart, L. Yang, H. Zhou, W. You, *J. Am. Chem. Soc*. 2011, **133**, 4625; c) C. Piliego, T. W. Holcombe, J. D. Douglas, C. H. Woo, P. M. Beaujuge, J. M. J. Fréchet, *J. Am. Chem. Soc.* 2010, **132**, 7595; d) H. Zhou, L. Yang, S. C. Price, K. J. Knight, W. You, *Angew. Chem. Int. Ed*. 2010, **49**, 7992.

Table of contents

Novel [60]fulleropyrrolidine derivatives were synthesized and evaluated based on device performance. The[60]fulleropyrrolidine derivatives with a phenyl group at the *N*-1 position of the pyrrolidine ring showed better photovoltaic performance than the *N*-alkyl derivatives. A power conversion efficiency of 7.34% obtained from the blend of the *N*-phenylfulleropyrrolidine derivative with a low-band-gap polymer is the world highest class performance among [60]fullerene-based OPV cells.

Keyword substituent effect; organic photovoltaic; fullerene derivative; *n*-type semiconductor

M. Karakawa, T. Nagai, K. Adachi, Y. Ie and Y. Aso*

N-Phenyl[60]fulleropyrrolidines: PC$_{61}$BM-Alternative Acceptor Material for High-Performance Organic Photovoltaic Cell